Molecular Therapy
Nucleic Acids
Original Article

Exon Skipping in a *Dysf*-Missense Mutant Mouse Model

Jakub Malcher,[1,2,7] Leonie Heidt,[1,4,7] Aurélie Goyenvalle,[2] Helena Escobar,[1,3] Andreas Marg,[1,4,5] Cyriaque Beley,[2] Rachid Benchaouir,[2] Michael Bader,[3,4,5,6] Simone Spuler,[1,3,4,5] Luis García,[2,8] and Verena Schöwel[1,3,5,8]

[1]Muscle Research Unit, Experimental and Clinical Research Center (ECRC), a cooperation between the Charité, Universitätsmedizin Berlin and the Max- Delbrück- Center for Molecular Medicine, 13125 Berlin, Germany; [2]Université de Versailles St-Quentin, INSERM U1179, 78180 Montigny-le-Bretonneux, France; [3]Max Delbrück Center for Molecular Medicine in the Helmholtz Association, 13125 Berlin, Germany; [4]Charité, Universitätsmedizin Berlin, 10117 Berlin, Germany; [5]Berlin Institute of Health, 10178 Berlin, Germany; [6]DZHK (German Centre for Cardiovascular Research), partner site, 13347 Berlin, Germany

Limb girdle muscular dystrophy 2B (LGMD2B) is without treatment and caused by mutations in the dysferlin gene (*DYSF*). One-third is missense mutations leading to dysferlin aggregation and amyloid formation, in addition to defects in sarcolemmal repair and progressive muscle wasting. Dysferlin-null mouse models do not allow study of the consequences of missense mutations. We generated a new mouse model (MMex38) carrying a missense mutation in exon 38 in analogy to a clinically relevant human *DYSF* variant (*DYSF* p.Leu1341Pro). The targeted mutation induces all characteristics of missense mutant dysferlinopathy, including a progressive dystrophic pattern, amyloid formation, and defects in membrane repair. We chose U7 small nuclear RNA (snRNA)-based splice switching to demonstrate a possible exon-skipping strategy in this new animal model. We show that Dysf exons 37 and 38 can successfully be skipped *in vivo*. Overall, the MMex38 mouse model provides an ideal tool for preclinical development of treatment strategies for dysferlinopathy.

INTRODUCTION

Dysferlin (*DYSF*, OMIM: 603009) is a 230 kDa large transmembrane protein highly expressed in skeletal muscle.[1] Dysferlin is found at the sarcolemma and in subsarcolemmal vesicles. Dysferlin is important in the wound healing of membranous microlesions in a calcium-dependent manner.[2–4] Mutations in the dysferlin gene (*DYSF*) cause limb girdle muscular dystrophy 2B (LGMD2B)[5] or the more distal forms, Miyoshi myopathy[6] and anterior tibial muscular dystrophy.[7] Currently, dysferlinopathies cannot be treated. Over 500 different disease-causing mutations have been described (Leiden Open Variation Database, last update March 31, 2017). One-third of those is missense mutations. Some of them exhibit typical characteristics of a protein-misfolding disease like protein aggregation, premature degradation, and amyloid formation.[8,9] We described a homozygous missense mutation *DYSF* c.4022T > C (p.Leu1341Pro) in exon 38 in a family of Arabic middle east origin with LGMD2B.[9] The mutation affects proper folding of the dysferlin C2E domain, and it leads to aggregate formation of non-functional protein.

All existing mouse models of dysferlinopathy, such as SJL/L, A/J, BLA/J, or Dysf-knockout mice, lead to a complete absence of dysferlin.[2,10–14] Consequences of a single amino acid variation and of protein misfolding could not be studied so far in an animal model.

Exon skipping is a therapeutic approach that uses short single-stranded nucleic acid analogs to mask specific motifs in pre-mRNA required for correct splicing. Antisense oligonucleotide (AON)-based splice-switching approaches have been developed for therapeutic use in human for Duchenne muscular dystrophy (DMD), spinal muscular atrophy,[15–20] and dysferlinopathy.[21,22] However, splice-modulating efficiency remains low in humans, and AONs must be repeatedly applied throughout life using invasive injection protocols, spurring research for more efficient and less invasive strategies. The U7 small nuclear RNA (snRNA)-encoded antisense RNAs differ from DNA-analog based AONs, in that they can easily be packaged into a suitable viral vector (i.e., recombinant adeno-associated virus [rAAV]) to transduce a wide variety of tissues, including skeletal muscle. U7 snRNA belongs to the group of minor snRNAs that take part in the processing of the 3′ end of histone pre-mRNA.[23] A native antisense sequence embedded in the U7 small nuclear ribonucleoprotein particle (snRNP) recognizes the 3′ UTR of histone transcripts[24,25] and can be modified for therapeutic purposes.[26–30] Therefore, AAV-U7 snRNA has several advantages over DNA analog chemistries, notably as bearing high transduction efficiency associated with strong and long-lasting antisense effect following a single systemic application.

Here we developed the first mouse model with a missense mutant in *Dysf*. The mutation was first described in patients (*DYSF* p.Leu1341Pro).[9] We designed a U7-based exon-skipping strategy and demonstrated the impact of exon removal on the dysferlin

Received 4 June 2018; accepted 16 August 2018;
https://doi.org/10.1016/j.omtn.2018.08.013.

[7]These authors contributed equally to this work.

[8]Senior author

Correspondence: Simone Spuler, Muscle Research Unit, Experimental and Clinical Research Center (ECRC), Lindenberger Weg 80, 13125 Berlin, Germany.
E-mail: simone.spuler@charite.de

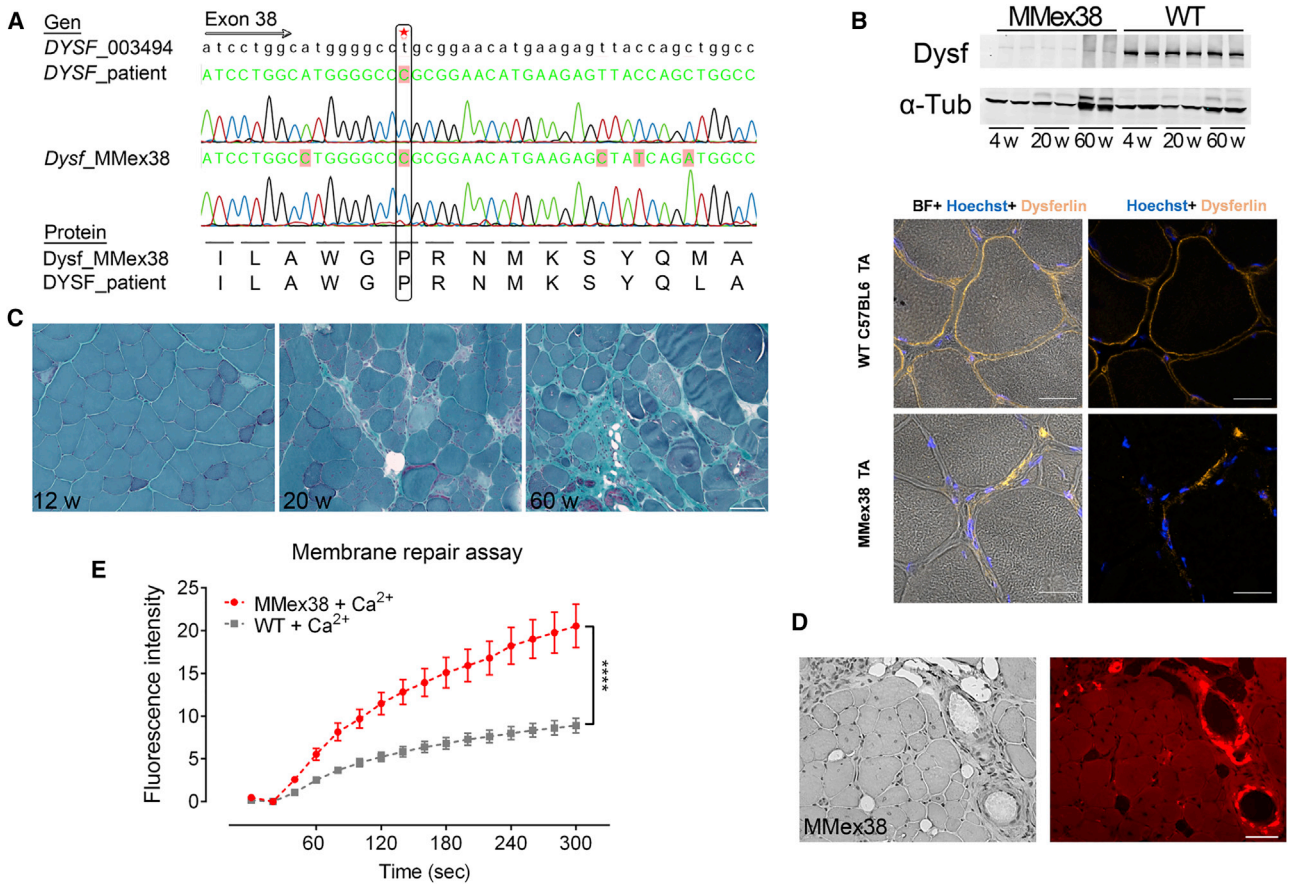

Figure 1. Characteristics of the New Animal Model Dysf-MMex38

(A) The index dysferlinopathy patient harbors the homozygous missense mutation *DYSF* c.4022T > C in exon 38. MMex38 mice carry the corresponding mutation *Dysf* c.4079T > C leading to *Dysf* p.Leu1360Pro (NCBI GenPept: NP_001071162.1, dysferlin isoform 2) (≙ *DYSF* p.Leu1341Pro, NM_003494) in the C2E domain (red asterisk) of dysferlin protein. (B) On the protein level, the missense mutated dysferlin detected by Hamlet antibody is markedly reduced (western blot of quadriceps muscle of differently aged mice; α-tubulin used as loading control). Dysf pLeu1360Pro does not localize at the membrane of MMex38 mice. Immunostaining of TA sections of MMex38 and WT mouse with Hoechst and Romeo antibody. Scale bars, 20 μm. (C) Dystrophic changes worsen with age in MMex38 mice (Gomori's trichrome staining of MMex38 quadriceps muscles). Scale bar, 50 μm. w, weeks of age. (D) Amyloid in MMex38 quadriceps muscle (Congo red staining). Scale bar, 50 μm. (E) Membrane repair after laser wounding is impaired in MMex38 flexor digitorum brevis muscle fibers (number of fibers n = 20 from 3 mice) compared to WT (number of fibers n = 24 from 4 mice) in the presence of Ca^{2+}. Fluorescence intensity below wounding site, mean ± SEM; ****p < 0.0001, unpaired t test for the time points above 300 s.

membrane repair activity. We prepared the molecular tools and viral vectors to deliver the splice-switching constructs *in vivo* and *in vitro*. We overcame the mutation by using AAV-U7 snRNA-mediated exon skipping in a novel mouse model for dysferlinopathy. The feasibility of the approach is demonstrated and technical limitations are discussed.

RESULTS

MMex38 Mice Display the Human Phenotype of Missense Mutant Dysferlinopathy

We generated a mouse model for missense mutant dysferlinopathy by introducing the murine mutation *Dysf* c.4079T > C (NCBI Genbank: NM_001077694.1) in exon 38 leading to p.Leu1360Pro (NCBI GenPept: NP_001071162.1, dysferlin isoform 2) (Figure 1A; Figure S1). Mice carrying the homozygous missense mutation are called MMex38 mice. The mutation is analogous to *DYSF* c.4022T > C (p.Leu1341Pro) in exon 38 causing LGMD2B.[9] The murine phenotype resembles the human disease progression and characteristics in several aspects. Newborn mice clinically and histopathologically do not display symptoms (data not shown). Signs of muscular dystrophy, such as necrotic and regenerating muscle fibers, fiber splitting, and fibrosis, first occurred in early adulthood (from week 12 onward) (Figure 1C; quantification and statistics are demonstrated in Figure S2), and they progressed significantly with age. At 60 months of age, more muscle fibers were replaced by fatty fibrosis (Figure 1C). Wild-type littermates of any age never showed pathological alterations in skeletal muscle.

On protein level *Dysf* p.Leu1360Pro led to a 90% reduction of dysferlin as assessed by western blot. Immunofluorescence stain for

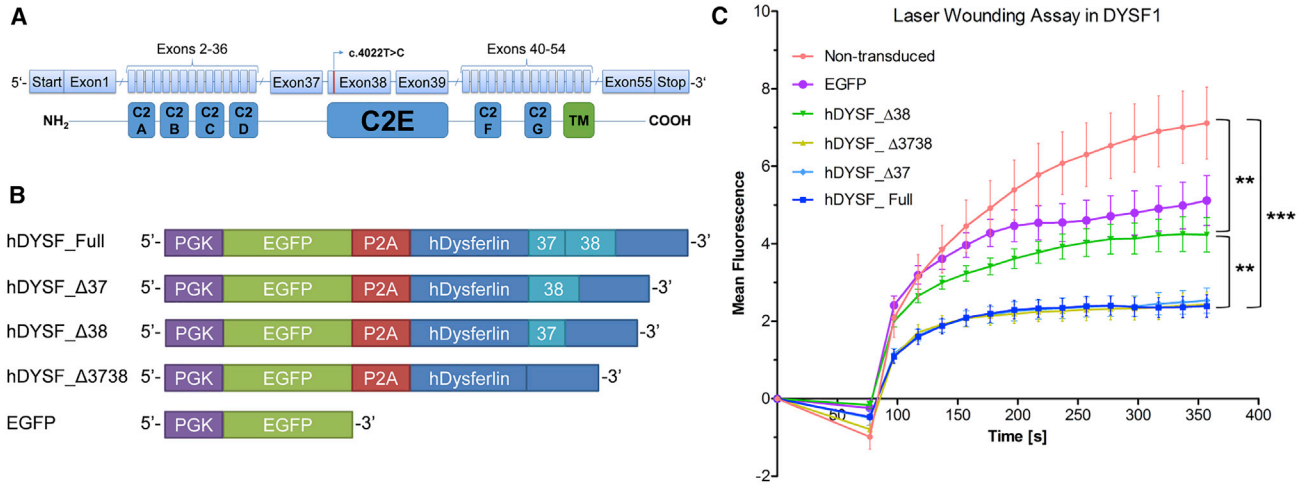

Figure 2. Functional Assessment of Exon 37- and 38-Truncated Dysferlin

(A) Schematic mapping of dysferlin domains on exons in pre-mRNA. (B) Dysferlin constructs introduced into dysferlin-null human myoblast via lentiviral transduction. (C) Quantification of the fluorescent signal influx into wounded myotubes over time. For each construct, the following number of myotubes was wounded: hDYSF_Δ37, n = 8; hDYSF_Δ38, n = 15; hDYSF_Δ3738, n = 14; hDYSF_Full, n = 15; non-transduced, n = 14; and EGFP, n = 7. Data points represent means ± SEM; **p < 0.01 and ***p < 0.001, unpaired t test for the time points above 350 s.

dysferlin on a frozen section revealed the absence of mutant dysferlin at the sarcolemma but occasional accumulations (Figure 1B).[9] As described for the patients carrying *DYSF* missense mutations,[8] MMex38 mouse muscle also displayed amyloid deposits at vessel walls (Figure 1D) and at the sarcolemma at older age.

To assess dysferlin function in MMex38 mouse muscle, we performed the laser-wounding assay on isolated muscle fibers from MMex38 flexor digitorum brevis muscle *ex vivo*. Membrane repair was significantly delayed in MMex38 as compared to wild-type (WT) littermates (Figure 1E), demonstrating that we had developed a fully functional dysferlin-missense mutant mouse model suitable for preclinical treatment attempts.

Dysferlin Devoid of Exons 37 and 38 Is Functional

We aimed to treat the *Dysf* c.4079T > C mutation by skipping the entire exon 38. We first needed to establish whether dysferlin lacking exon 38 would be functional. According to UniProt database annotation, exon 38 and exon 39 encode dysferlin C2E domain (UniProt: O75923) (Figure 2A).[31] The length of the intron between exons 37 and 38 is only 118 nt, a distance that might be too short to interfere efficiently with the splicing machinery by means of a splice-switching strategy. We therefore also considered combined removal of exons 37 and 38. We cloned four human *DYSF* variants, and we expressed them via lentiviral transduction in primary human myoblast cells carrying a dysferlin null mutation (homozygous *DYSF* c.4872delG): full *DYSF* (hDYSF_Full), *DYSF* without exon 37 (hDYSF_Δ37), *DYSF* without exon 38 (hDYSF_Δ38), and *DYSF* without exons 37 and 38 (hDYSF_Δ3738) (Figure S3). All constructs were linked to an EGFP reporter via P2A (Figure 2B) to enable sorting for transduced cells (Figure S4A). Sorted myoblasts were differentiated into myotubes, and dysferlin expression was verified by immunostaining of dysferlin-null myotubes (Figure S4B). The membrane-wounding assay was used to demonstrate functional outcomes (Figure S5).[2,3]

Non-transduced DYSF-null myotubes and myotubes infected with GFP only showed the highest fluorophore uptake, demonstrating the expected delay in repairing minute sarcolemmal lesions in dysferlinopathy (Figure 2C). Myotubes transduced with full-length *DYSF* normalized the membrane repair time (Figure 2C). hDYSF_Δ37 and hDYSF_Δ3738 demonstrated the same resealing performance as hDYSF_Full. Transduction with hDYSF_Δ38 resulted in an only incomplete membrane resealing, confirming our predicted caution of deleting exon 38 only. Our data demonstrate that the partial deletion of the C2E domain by simultaneous removal of both exons 37 and 38 restores dysferlin protein function in patient-derived dysferlin-null cells. These results provide the rationale underlying a therapeutic strategy aimed at skipping mutated exons 37–38 in patients experiencing dysferlinopathies with a missense mutation in exon 38.

U7 snRNA Antisense Sequences Skip Mouse Dysferlin Exons 37 and 38 in MDX Muscles *In Vivo* and in C2C12 Cells *In Vitro*

Pre-mRNA splicing is a highly complex machinery that involves interaction between multiple RNA-binding proteins with a wide spectrum of splicing silencers and enhancers.[32] We used the relative enhancer and silencer classification by unanimous enrichment (RESCUE)-ESE algorithm to predict localization of potential exonic splice enhancers (ESEs) in the mouse *Dysf* exon 37 and 38 sequence.[33,34] We designed 12 antisense sequences spanning exon 38 and parts of neighboring introns of *Dysf* pre-mRNA (Figure 3A; Table S1), based on their ability to mask exon 38 (U2.7, U4.7, U6.5, U7.10, U8.2, U9.2, and U10.1), to target the intron 37–38 branching

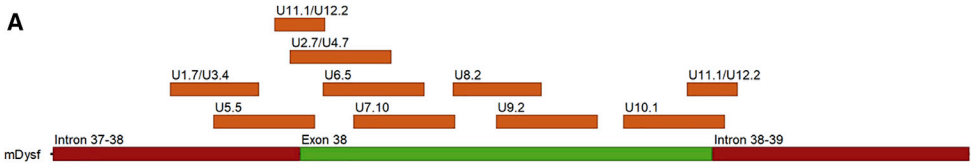

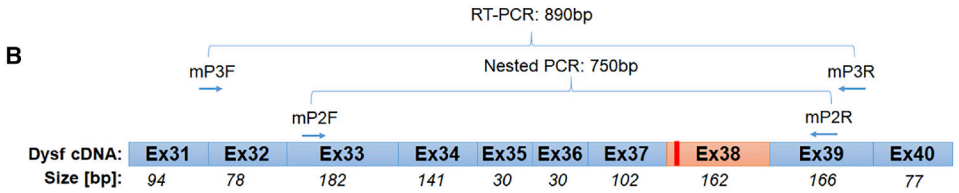

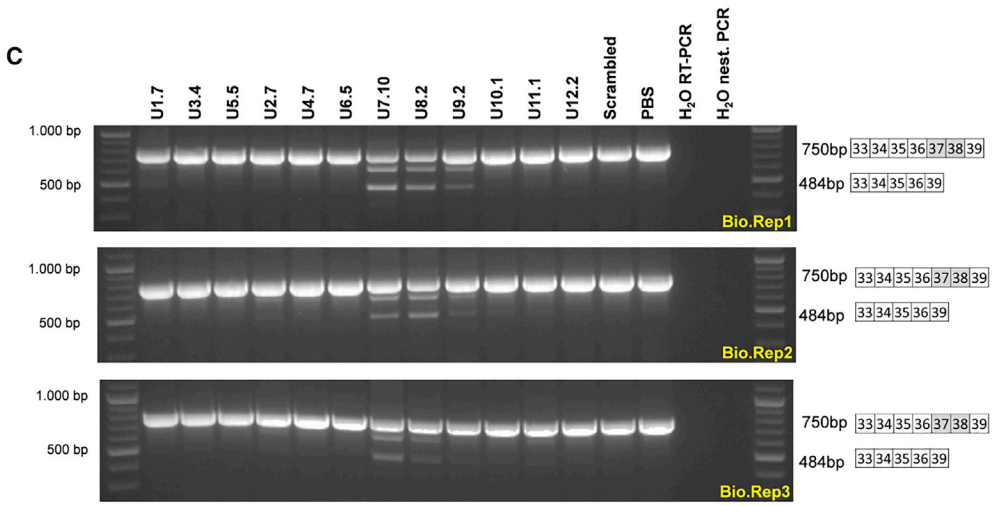

D

Densitometry	ex37&38 Skipping Level		
	U7.10	U8.2	U9.2
Repeat 1	29%	24%	6%
Repeat 2	8%	15%	3%
Repeat 3	12%	6%	2%
Average	16%	15%	4%

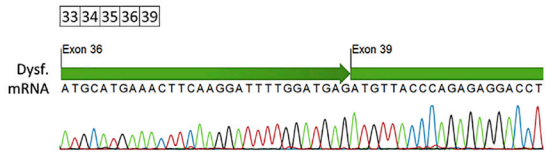

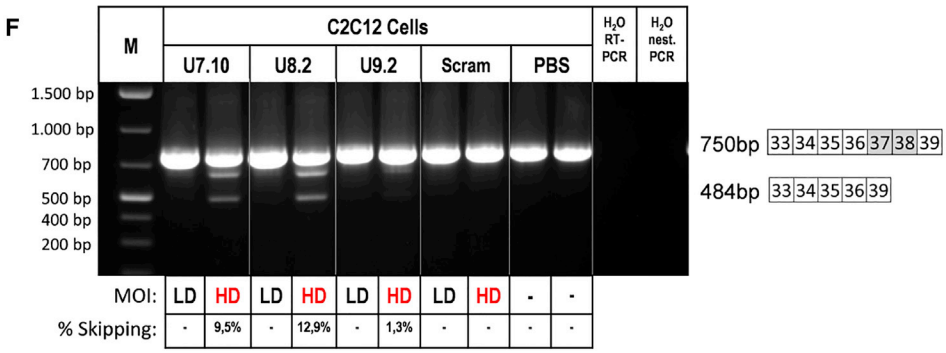

(legend on next page)

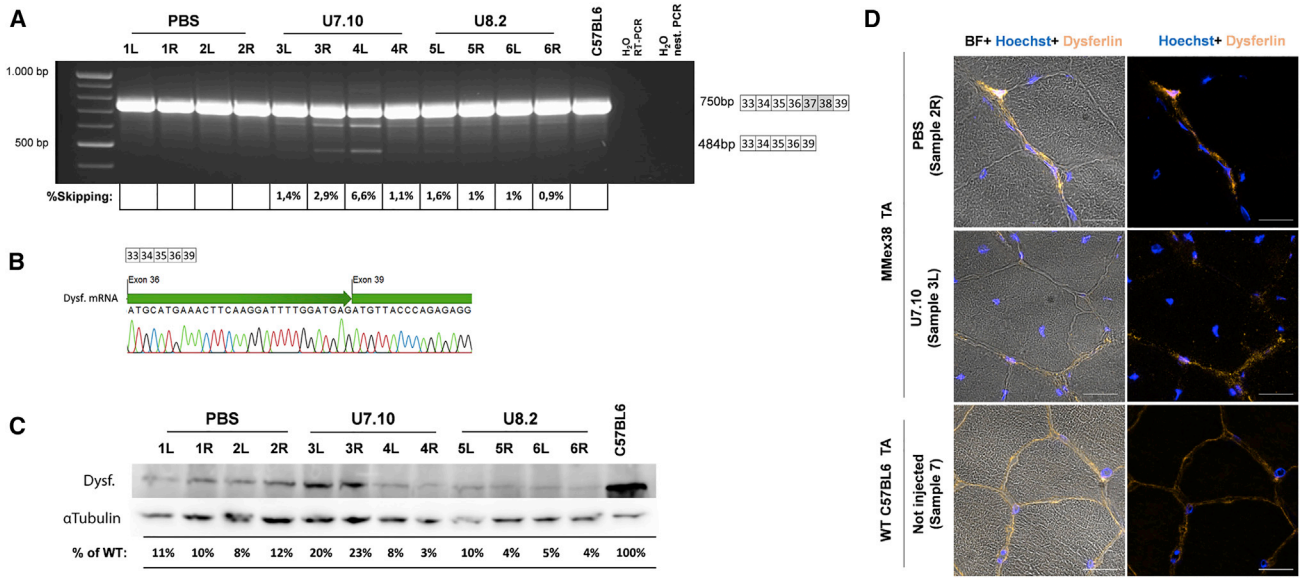

Figure 4. U7-Based Exon Skipping in MMex38 Mice

(A) Detection of exon skipping using RT-PCR and nested PCR for dysferlin mRNA spanning the region between exons 33 and 39. Densitometric quantification of exon skipping in MMex38 mice using ImageJ is shown. (B) Sequencing of the skipped dysferlin. The presence of the junction between the exons 36 and 39 was verified. (C) Detection of dysferlin expression in MMex38 TAs treated with U7 snRNAs using biotin-streptavidin western blot with Hamlet antibody (α-tubulin as loading control). Densitometric quantification of dysferlin as a percentage of WT (C57BL6) using ImageJ is shown. (D) Immunostaining with Hoechst and Romeo antibody of TA sections of MMex38 treated with U7 snRNAs and WT mouse treated with PBS. Scale bars, 20 μm.

point (U1.7, U3.4, and U5.5), or to cover the acceptor splice site of intron 37–38 (U2.7, U4.7, and U5.5). One sequence was designed to target the donor site of intron 38–39 (U10.1). U11.1 and U12.2 masked both the acceptor site of intron 37–38 and the donor site of intron 38–39. The sequence pairs U1.7/U3.4, U2.7/U4.7, and U11.1/U12.2 masked the same regions of the mouse *Dysf* pre-mRNA, but the rationale was to optimize the antisense sequences to contain a nucleotide matching the so-called kiss domain.[35] We could not detect an advantage of this approach in our study. The secondary structure of all U7 snRNAs was analyzed using RNAfold[36] to exclude the existence of hairpin structures. The U7 snRNA constructs were packaged into rAAV2/9 viruses.

We first tested the suitability of our U7 snRNAs in 10-week-old MDX mice. This mouse has been characterized extensively, and it has been used for preclinical assessment of new treatment strategies. It displays necrosis and regeneration of muscle fibers due to muscular dystrophy. We injected each U7 construct into the anterior tibial muscle of MDX mice. Three antisense sequences (U7.10, U8.2, and U9.2) effectively induced exon skipping, as detected by RT-PCR and nested PCR 4 weeks after delivery (Figures 3B and 3C). All of the successful U7 snRNAs simultaneously deleted both exons 37 and 38. The results were confirmed by sequencing (Figure 3E). Skipping efficacy was 15%–16% for U7.10 and U8.2 and 4% for U9.2 (Figure 3D). We also compared our *in vivo* experiments to *in vitro* attempts using the universal murine muscle cell line C2C12. We could confirm that also in the *in vitro* model the U7.10 and U8.2 were the best performing antisense sequences and U9.2 was the least efficient one (12.9%) (Figure 3F).

U7 snRNA Antisense Sequences Skip Mouse Dysf Exons 37 and 38 in MMex38

We used the most potent rAAV2/9-U7 snRNAs (U7.10 and U8.2) from MDX and C2C12 experiments to trigger exon skipping *in vivo* in MMex38 mice, using the same transduction protocol (1.2×10^{11} vector genomes [VG] per tibialis anterior [TA]). MMex38 mice were 8 weeks of age and did not show any signs of muscular dystrophy yet. Analysis also was performed 4 weeks after the injection. U7.10 and U8.2 triggered simultaneous skipping of exons 37 and 38 (Figures 4A and 4B). Single exons were not skipped. The overall skipping efficiency reached 6.6% (Figure 4A). On the protein level, an increase in dysferlin expression to a level of about 20% of the WT was observed

Figure 3. Screening of U7 snRNA Antisense Sequences for Exon-Skipping Activity in MDX Mice and C2C12 Cells

(A) Antisense sequences of U7 snRNA constructs mapped on the intron 37–38, exon 38, and intron 38–39 of mouse dysferlin pre-mRNA. (B) Primer localization. (C) Detection of exon skipping using RT-PCR and nested PCR in MDX mice. The intermediate-sized bands represent a heteroduplex formed between the full and skipped PCR product.[53] (D) Densitometric quantification of exon skipping in MDX mice. (E) Sequencing of the skipped dysferlin. The presence of the junction between exons 36 and 39 was verified. (F) Detection and densitometric quantification of exon skipping using RT-PCR and nested PCR in C2C12 cells. LD, low dose; HD, high dose.

for two TAs injected with the U7.10 antisense sequence (Figure 4C). In immunostaining of sample 3L, we were able to detect a very small amount of additional membrane-bound dysferlin (Figure 4D).

DISCUSSION

We generated MMex38 mice, the first mouse model of dysferlinopathy with a *Dysf* missense mutation rather than the complete knockout models described thus far.[2,10–14] The mutation closely resembles a clinically relevant mutation also present in a cohort of patients.[8] We succeeded to skip the mutation-containing exon by U7 snRNA-mediated exclusion, and we demonstrate that dysferlin after removal of exons 37 and 38 is functional.

Up to now, few muscular dystrophy mouse models exist carrying disease-specific missense mutants. Many attempts failed to reproduce a clinical phenotype in mice.[37,38] A missense mutant of a gene encoding for a sarcolemmal protein allows for gene editing, for interference with protein folding and degradation, as well as for exploring overarching concepts of how membrane integrity could be maintained in muscular dystrophy.

Exon-skipping strategies are one of the most promising approaches for muscular dystrophies and could be particularly useful to eliminate mutations. Exon skipping is generally induced by antisense oligonucleotides. However, there are several reasons why U7 snRNAs might be preferable. Once delivered to tissue, U7 snRNAs can be expressed constantly without the need for a repeated administration as is the case with the synthetic antisense oligonucleotides. Furthermore, embedding the antisense sequences into the U7 snRNA with an optimized Sm protein-binding site assures their accumulation in the nucleus,[39,40] and it increases the probability of modifying the constitutive splicing process. The U7 snRNA can be packaged into rAAV and lentiviruses for an efficient and tissue-specific delivery. They also can be combined with a cell therapy strategy to produce primary cells expressing splice-switching molecules for later tissue transplantation.[41] In addition, U7 snRNA can be further modified with sites for binding splicing repressor proteins to create a bifunctional snRNA with enhanced skipping activity.[42] Indeed, the U7 RNA approach for exon skipping has been proven to be efficient and successful in dystrophinopathy. Dystrophin expression in the MDX mouse model,[29] dystrophin-utrophin knockout mice,[43] and also in large animals[44,45] remarkably improved following treatment with the AAV-U7 snRNA. Based on these promising results, clinical trials are presently being designed and prepared.

In vivo skipping efficacy of exons 37 and 38 in MMex38 mice reached only 6.6% compared to 16% using the same U7 snRNA in the MDX mice. There are several possibilities that could explain this discrepancy. The lack of dysferlin at the sarcolemma in MMex38 mice could have an impact on viral transduction efficiency into the fiber. Alternatively, the difference might have arisen from the fact that, in the case of MMex38 mice, a healthy presymptomatic muscle was treated, whereas in the MDX model the muscle was in constant cycles of necrosis and regeneration. Viral uptake may be facilitated during regeneration. It is a peculiarity of dysferlinopathies that patients and mice are free of symptoms and myopathological alterations until adulthood. We identified the first histological signs of a muscular dystrophy in 12-week-old MMex38 mice, but exon-skipping treatment was initiated at 8 weeks of age. There is a good rationale to initiating treatment as early as possible and even performing a screening for muscular dystrophies in newborns.[46] However, apart from ethical questions, our findings of inferior treatment efficacy in a presymptomatic setting adds another aspect to this discussion.

It is estimated that only small amounts of dysferlin are required to promote functionality and to prevent progressive muscle loss.[12] It is, therefore, possible that skipping efficacy of 6%–7% maximally as shown here might be sufficient to interfere with the course of the disease. On the mRNA level, U7.10 4L resulted in the best skipping efficiency, and on the protein level the highest dysferlin expression was seen in U7.10 3L and 3R. This discrepancy is attributed to both muscle sampling from different parts of TA and uneven distribution of AAV after an intramuscular injection. Only future experiments designed to treat the entire animal rather than a single muscle will be able to estimate the success of our approach. Optimization of the exon-skipping tool would be also required. For instance, new antisense sequences might trigger a stronger exon-skipping effect. Use of bifunctional U7 snRNAs,[42] which contain both antisense sequence and a splice enhance sequence, could be another option for improving the skipping efficiency.

MATERIALS AND METHODS

Animal Work

The MMex38 mice were kept at the Animal Facility of Max Delbrück Center for Molecular Medicine, Berlin. All experiments performed in Berlin were approved by the local governmental authority (Landesamt für Gesundheit und Soziales Berlin, Germany). Breeding and characterization of the MMex38 mouse strain were performed under the licenses G0065/13 and G0257/14, and exon-skipping experiments were under the license G0145/16. The exon-skipping experiments with MDX mice were performed in France at UFR des sciences de la santé Simone Veil-Université de Versailles Saint-Quentin-en-Yvelines under the license APAFIS6518-2016081715535828 v2 from the Ministère de l'Enseignement supérieur de la Recherche et de l'Innovation.

MMex38 Mouse Model Generation

Three homological arms of genomic *Dysf* were derived by PCR from embryonic stem cell (ESC) DNA of the 129 strain. The target T > C mutation in *Dysf* exon 38 leading to Dysf p.Leu1360Pro (dysferlin isoform 2, NCBI GenPept: NP_001071162.1) was introduced by site-directed mutagenesis. The targeting vector consisted of a 4.8-kb-long 5′-targeting arm, including genomic DNA spanning from *Dysf* intron 36 to exon 38 (5′ long homology arm), a 150-bp 5′ short targeting arm containing genomic DNA from *Dysf* exon and intron 38 (5′ short homology arm), and a 3′-targeting arm containing 1.5 kb of genomic DNA from intron 38 (3′ homology arm) (Figure S1). The targeting vector included a LoxP site-flanked

neomycin resistance cassette (Neo) (between cloned sequences of the 5′ short and 3′ homology arms, flanked by genomic sequence of *Dysf* intron 38). Primers are listed in Table S2. The plasmid was confirmed by sequencing.

After linearization, we performed electroporation, and the targeting construct was inserted by homologous recombination into ESCs (129ola). Cells were initially selected via their neomycin resistance. We confirmed correct genomic insertion by PCR and sequencing. We used correctly targeted ESCs to perform microinjection into C57BL/6 blastocysts and generate knockin mice using standard techniques (Transgenic Core Facility, Max Delbrück Center for Molecular Medicine, Berlin). The MMex38 strain was generated by crossing transgenic animals with a ubiquitous Cre deleter mouse strain. The founder line was backcrossed on a C57BL/6N genetic background 5 times before mouse model characterization was performed (B6;129P2-Dysf$^{tm1.1Mdcb}$). In all experiments WT littermates served as controls. Mice were genotyped by PCR of ear-tag DNA using AmpliTaq Gold 360 DNA Polymerase (Thermo Fisher Scientific, Darmstadt, Germany), and primers are listed in Table S3 as well as illustrated in Figure S1.

Histochemistry and Histopathology

Trichrome and Congo red staining were performed according to standard protocols. Images were collected using either the Leica DMI6000 (Leica Microsystems, Wetzlar, Germany) or the Zeiss LSM 700 confocal microscope (Carl Zeiss, Germany). Digital images were processed using the LAS AF software (Leica) or the Zeiss LSM ZEN software (Carl Zeiss, Jena, Germany). Quantification of histopathology was performed counting the number of regenerating fibers, necrotic fibers, and fibers with centralized nuclei per 100 fibers. Fiber diameter was determined using ImageJ software (Wayne Rasband, NIH, Bethesda, MD, USA).

Membrane Repair Assay of Single Muscle Fibers and Dysferlin-Null Primary Human Myotubes

Flexor digitorum brevis muscle was isolated and dissolved in minimum essential medium (MEM), fetal calf serum (FCS, 10%), and collagenase 1 for 3 hr at 37°C. Under the microscope, connective tissue and vessels were removed and muscle fibers were gently separated. By pipetting, single muscle fibers were isolated from the fiber bundle and fixated on laminin-coated atomic force microscopy (AFM) basins with MEM, FCS (10%), and gentamycin (= Complete MEM) overnight. Fibers were washed with Tyrode solution (5 mM KCl, 140 mM NaCl, 2 mM $MgCl_2$, 2.5 mM $CaCl_2$, and 10 mM HEPES [pH 7.2]).[3] 2.5 μM FM1-43 fluorescent dye was added to the fibers. Laser wounding was performed by irradiation of an area of 5 × 5 μm at the fiber membrane using all four lasers of the Zeiss LSM 700 laser microscope with a total power of 30 MW. Myoblasts were differentiated in 3.5-cm glass-bottom dishes (ibidi, Martinsried, Germany). The assay was performed in 1 mL Tyrode solution supplemented with 2.5 μL 1 mM FM4-64 fluorophore (Invitrogen, Darmstadt, Germany). Myotubes were wounded by irradiating a membranous area of 2.5 × 2.5 μm for 60 s. In both experimental settings, a single image was taken before irradiation and further pictures were recorded in time series every 20 s after wounding to observe the changes in the fluorescence intensity over time. Fluorescent intensities were measured using ImageJ software (Wayne Rasband, NIH, Bethesda, MD, USA).

Western Blot

The muscle tissue was dissolved in 50 mM Tris, 150 mM NaCl, 0.5% Triton X-100, 0.5% Na-Deoxycholate, 1 mM EDTA, 50 mM NaF, 1 mM Na_3VO_4, 1 mM PMSF, and 1× Complete (Roche, Mannheim, Germany) for 30 min; centrifuged for 15 min (13,200 rpm); and the supernatant was collected. Antibodies used for western blot were mouse anti-dysferlin mab HAMLET (Novocastra, Wetzlar, Germany), rabbit anti-dysferlin mab ROMEO (ab124684, Abcam), and mouse α-tubulin mab T5168 (Sigma-Aldrich, St. Louis, MO, USA). For the biotin-streptavidin detection system, a biotin-conjugated secondary antibody donkey anti-mouse (Dianova, Hamburg, Germany) together with high-sensitivity streptavidin-horseradish peroxidase (HRP) (Thermo Fisher Scientific, Rockford, IL, USA) was used. Western blots were detected by chemiluminescence (Amersham ECL Advance Western Blotting Detection Kit; GE Healthcare) or by the ODYSSEY infrared imaging system (LI-COR Biosciences, Lincoln, NE, USA).

Cell Culture and Differentiation into Myotubes

The human primary myoblasts and C2C12 cells were cultured in a humidified incubator at 37°C with 5% CO_2 in in Skeletal Muscle Cell Growth Medium (Provitro, Berlin, Germany) containing 15% FCS, fetuin, human recombinant epidermal growth factor (hEGF), human recombinant fibroblast growth factor (bFGF), insulin, dexamethasone, gentamicin, and amphothericin B and enriched with 1× glutamax (Life Technologies). For differentiation of human primary myoblasts or C2C12, cells were grown up to 70% confluency and the medium was changed to Opti-MEM reduced serum medium (Life Technologies) supplemented with 2% horse serum (Lonza, Basel, Switzerland).

Immunostainings

Transversal muscle tissue cryosections of 6 μm were fixed for 5 min in acetone at −20°C and blocked with 1% BSA in PBS for 45 min at room temperature. Sections were incubated overnight at 4°C with the primary ROMEO anti-Dysferlin rabbit monoclonal antibody (Abcam, Cambridge, UK, 1:100). Sections were incubated with the secondary goat anti-rabbit Cy3-conjugated antibody (Dianova, Hamburg, Germany, 1:500) for 45 min at room temperature. Nuclei were stained with Hoechst. The sections were mounted with AquaMount (Polysciences, Hirschberg, Germany). Cells were seeded on glass-bottom plates (ibidi, Martinsried, Germany) and fixed with 3.7% formaldehyde for 10 min at room temperature. Cells were permeabilized with 0.2% Triton X-100 in PBS for 5 min at room temperature. Cells were blocked with 1% BSA in PBS for 1 hr at room temperature and incubated overnight at 4°C with two primary antibodies: mouse monoclonal antibody anti-Desmin (Dako, Jena, Germany; 1:100) and rabbit monoclonal antibody ROMEO

anti-Dysferlin (Abcam, 1:150). Cells were incubated for 1 hr at room temperature with the following secondary antibodies (both diluted to 1:500): polyclonal Alexa 568 donkey anti-rabbit (Life Technologies) and polyclonal Alexa 647 goat anti-mouse (Life Technologies). Nuclei were stained with Hoechst.

Cloning of Dysferlin Constructs

The four versions of dysferlin protein (hDYSF_Full, hDYSF_Δ37, hDYSF_Δ38, and hDYSF_Δ3738) connected to EGFP via P2A peptide were made from the plasmids containing full-length human dysferlin cDNA pUC57-Kan-DysfFull and truncated human dysferlin cDNA pUC57-Kan-DysfΔex37 and pUC57-Kan-DysfΔex38, obtained as a gift from the Jain Foundation. The pUC57-Kan-DyfΔex37&38 plasmid was constructed using whole-plasmid PCR with Phusion Master Mix (Thermo Fisher Scientific) and P11cF, P11aR primers (Table S4). For further clonining, the dysferlin cDNA was amplified with c25F, c25R and c26F, c26R primers. The P2A sequence was obtained from lentiCRISPR v2, which was a gift from Feng Zhang (Addgene plasmid 52961).[47] The dysferlin constructs were connected to EGFP and P2A via PCR reactions with the cP23F, cP23R, cP24F, cP24R, and DYSF-Seq1R primers (Table S4), and they were cloned into the pRRLSIN.cPPT.PGK-MCS.WPRE plasmid used for the lentivirus production. The constructs were verified by sequencing.

Lentivirus Production

Third-generation,[48] self-inactivating lentiviral vectors[49] were produced in the L.G. laboratory at Université de Versailles Saint-Quentin-en-Yvelines, France, using quadri-transfection of 293T cells. Sequences encoding Gag, Pol, and Rev proteins were delivered on pMDLg/pRRE and pRSV-Rev packaging plasmids, whereas the vesicular stomatitis virus envelope glycoprotein (VSV-G) was delivered on pMD2.G plasmid. The viral long terminal repeats (LTRs) with dysferlin gene connected to EGFP and under the control of human phosphoglycerate kinase-1 (PGK-1) promoter were delivered on the pRRLSIN.cPPT.PGK-MCS.WPRE plasmid. At 3 days after transfection of 293T cells, the supernatant was collected and centrifuged at 3,500 × *g* for 30 min and filtered via a 0.3-μm filter. The filtered supernatant was further concentrated using tangential flow filtration system from Specturm Labs. The concentrate was centrifuged for 2 hr at 20,000 rpm with Beckmann ultracentrifuge, and the viral pallet was resuspended in PBS, aliquoted, and frozen at −80°C. Viral titer was estimated by means of Lenti-X qRT-PCR Titration Kit (Clontech Laboratories, Saint-Germain-en-Laye, France) and titration by infection using flow cytometry.

Lentiviral Transduction of Dysferlin-Null Myoblasts with Dysferlin Constructs and FACS

Dysferlin-null human primary myoblasts (exon 44: c.4872delG) were transduced with lentivirus carrying full and truncated dysferlin constructs at an MOI of 2. The cells were seeded at the density of 25,000 cells/well. The next day the cells were washed with PBS and medium was changed. An appropriate amount of virus was added. The cells were inoculated with the virus for 24 hr and afterward cultured to obtain enough cells for fluorescence-activated cell sorting (FACS). The cells were stained with the primary mouse monoclonal antibody anti-CD56-NCAM (Miltenyi Biotec, Bergisch Gladbach, Germany) 1:200 in combination with the secondary Alexa 647 goat anti-mouse antibody (Invitrogen) 1:500. The cells were sorted using BD FACSaria F cell sorter to enrich for the myoblast population expressing high levels of EGFP signal.

Cloning of Antisense Sequences into U7 snRNA Backbone

The U7 snRNA backbone was modified using cP21_F, cP21_R and XbaI_F, NheI_R primers (Table S4) in order to introduce the BbsI and EcoRI restriction sites for later cloning of the antisense sequences. The U7 antisense sequences were ordered at Eurogentech, Seraing, Belgium, as two complementary single-stranded oligonucleotides with BbsI overhangs at the 5′ and 3′ ends. The pSMD2-U7-BbsI plasmid was digested with BbsI restriction enzyme (New England Biolabs), and the annealed antisense oligonucleotides were cloned into the vector. The correctness of U7 antisense sequence was verified by sequencing.

rAAV Production

The rAAV2/9 for the test in MDX mice was produced in the L.G. laboratory at Université de Versailles Saint-Quentin-en-Yvelines, France. The production was done using the tri-transfection method[50] combined with the downstream detergent treatment, according to the protocol of Dias Florencino and colleagues.[51] For tri-transfection, a plasmid pAAV2/9 encoding replication and capsid proteins, a helper plasmid pXX6, and a transgene encoding plasmid pSMD2 were used. The rAAV2/9 for the C2C12 cell experiment was produced in the L.G. laboratory at Université de Versailles Saint-Quentin-en-Yvelines, France, using the baculovirus expression system in SF9 insect cells, according to the Buclez et al.[52] protocol. The rAAV2/9 titers for all productions were estimated by qPCR. The rAAV2/9 for the *in vivo* injections into MMex38 was produced using the tri-transfection method and titrated at Charite Viral Core Facility in Berlin, Germany.

Transduction of AAV-U7 snRNAs into C2C12 Cells

The C2C12 cells were seeded at the density of 500,000 cells/well in a 6-well plate. The next day the cells were washed with PBS and medium was changed. 5×10^{11} VG for a low dose and 5×10^{12} VG for a high dose of AAV-U7 snRNAs were added, and the cells were inoculated with the virus for 24 hr. Next the medium was changed to a differentiation medium (DMEM, 2% horse serum, 1% PenStrep), and the cells were differentiated for 5 days.

Intramuscular Injections of AAV-U7 snRNAs into the TA Muscle of Mice

The U7 snRNAs packaged in rAAV2/9 and dissolved in PBS were delivered as an intramuscular injection into the TA muscle at the amount of 1.2×10^{11} VG/TA for the MMex38 mice and 1.32×10^{11} VG/TA for the MDX mice. For this purpose, 2-month-old MMex38 mice and 2.5- or 3-month-old MDX mice were anesthetized by inhalation of 2% isoflurane, hind limbs were shaved, and

injections were made with an insulin syringe. The mice were sacrificed by cervical dislocation 4 weeks after the injection, and the muscle was harvested for the analysis.

RNA Isolation and RT-PCR Analysis

Total RNA was isolated from cells or mouse TA muscle using TRIzol Reagent (Life Technologies), according to the manufacturer's protocol. For the RNA isolation, the muscle samples were homogenized in Precellys24 (Bertin Instruments, Montigny-le-Bretonneux, France) at 5,000 rpm for 45 s and at 6,800 rpm for 15 s. RNA was resuspended in RNase-free water, incubated in heat block at 55°C for 15 min, and finally stored at −80°C. Between 0.5 and 1 μg total RNA was used in a reverse transcription reaction. For the detection of exon skipping, the reverse transcription and PCR reactions were done using Access-Quick RT-PCR System (Promega, Mannheim, Germany) using a pair of external primers, mP3F (5′-TCTTTGACTATGGGAACCGCT-3′) and mP3R (5′-CTGTGGGGATGGACTCTCTG-3′). 2 μL PCR product and a pair of internal primers, mP2F (5′-AAGCCAGAAGACAG TGGTGG-3′) and mP2R (5′-GAGTATGGGTCGCACAGGAA-3′), were taken for the nested PCR reaction using GoTaq Master Mix (Promega). The nested PCR product was analyzed for the skipped exons on an agarose gel. The level of exon skipping was estimated by densitometry method using ImageJ (Wayne Rasband, NIH, Bethesda, MD, USA) quantification.

SUPPLEMENTAL INFORMATION

Supplemental Information includes five figures and four tables and can be found with this article online at https://doi.org/10.1016/j.omtn.2018.08.013.

AUTHOR CONTRIBUTIONS

V.S. and M.B. designed and created the MMex38 mouse model. V.S. and L.H. characterized the MMex38 mouse model. J.M. designed the exon-skipping strategy, performed cloning, produced lenti and AAVs vectors, designed and performed functional study on truncated dysferlin, and carried out exon-skipping experiments *in vitro* and *in vivo*. A.G. performed MDX mouse injections and provided supervision and strategic guidelines for U7-based experiments. H.E. performed FACS of human primary myoblasts and helped with the satellite cell isolation. A.M. and V.S. provided experimental and strategic guidelines for laser-wounding experiments. C.B. helped with the design of cloning strategies and provided experimental guidelines for the cloning tasks. R.B. provided experimental and strategic guidelines for the production of lentiviruses and rAAVs. S.S., L.G., V.S., and J.M. designed the experiments and wrote the manuscript.

CONFLICTS OF INTEREST

The authors have no conflict of interest.

ACKNOWLEDGMENTS

The study was supported by the German Research Foundation (DFG) through the International Research Training Group for Muscle Sciences "MyoGrad" IGK1631 with grants to J.M., L.G., and S.S.; the Helmholtz Association through a KAP-stipend to V.S.; and Charité Universitätsmedizin Berlin through a doctoral student stipend to L.H. The study was also supported by the Duchenne Parent project France and the Association Monégasque contre les Myopathies. We also acknowledge support from the Open Access Publication Fund of Charité – Universitätsmedizin Berlin. We thank all patients for their interest and their contribution to our research.

REFERENCES

1. Anderson, L.V., Davison, K., Moss, J.A., Young, C., Cullen, M.J., Walsh, J., Johnson, M.A., Bashir, R., Britton, S., Keers, S., et al. (1999). Dysferlin is a plasma membrane protein and is expressed early in human development. Hum. Mol. Genet. *8*, 855–861.

2. Bansal, D., Miyake, K., Vogel, S.S., Groh, S., Chen, C.-C., Williamson, R., McNeil, P.L., and Campbell, K.P. (2003). Defective membrane repair in dysferlin-deficient muscular dystrophy. Nature *423*, 168–172.

3. Marg, A., Schoewel, V., Timmel, T., Schulze, A., Shah, C., Daumke, O., and Spuler, S. (2012). Sarcolemmal repair is a slow process and includes EHD2. Traffic *13*, 1286–1294.

4. Bansal, D., and Campbell, K.P. (2004). Dysferlin and the plasma membrane repair in muscular dystrophy. Trends Cell Biol. *14*, 206–213.

5. Bashir, R., Britton, S., Strachan, T., Keers, S., Vafiadaki, E., Lako, M., Richard, I., Marchand, S., Bourg, N., Argov, Z., et al. (1998). A gene related to Caenorhabditis elegans spermatogenesis factor fer-1 is mutated in limb-girdle muscular dystrophy type 2B. Nat. Genet. *20*, 37–42.

6. Miyoshi, K., Kawai, H., Iwasa, M., Kusaka, K., and Nishino, H. (1986). Autosomal recessive distal muscular dystrophy as a new type of progressive muscular dystrophy. Seventeen cases in eight families including an autopsied case. Brain *109*, 31–54.

7. Illa, I., Serrano-Munuera, C., Gallardo, E., Lasa, A., Rojas-García, R., Palmer, J., Gallano, P., Baiget, M., Matsuda, C., and Brown, R.H. (2001). Distal anterior compartment myopathy: a dysferlin mutation causing a new muscular dystrophy phenotype. Ann. Neurol. *49*, 130–134.

8. Spuler, S., Carl, M., Zabojszcza, J., Straub, V., Bushby, K., Moore, S.A., Bähring, S., Wenzel, K., Vinkemeier, U., and Rocken, C. (2008). Dysferlin-deficient muscular dystrophy features amyloidosis. Ann. Neurol. *63*, 323–328.

9. Wenzel, K., Carl, M., Perrot, A., Zabojszcza, J., Assadi, M., Ebeling, M., Geier, C., Robinson, P.N., Kress, W., Osterziel, K.J., and Spuler, S. (2006). Novel sequence variants in dysferlin-deficient muscular dystrophy leading to mRNA decay and possible C2-domain misfolding. Hum. Mutat. *27*, 599–600.

10. Weller, A.H., Magliato, S.A., Bell, K.P., and Rosenberg, N.L. (1997). Spontaneous myopathy in the SJL/J mouse: pathology and strength loss. Muscle Nerve *20*, 72–82.

11. Bittner, R.E., Anderson, L.V.B., Burkhardt, E., Bashir, R., Vafiadaki, E., Ivanova, S., Raffelsberger, T., Maerk, I., Höger, H., Jung, M., et al. (1999). Dysferlin deletion in SJL mice (SJL-Dysf) defines a natural model for limb girdle muscular dystrophy 2B. Nat. Genet. *23*, 141–142.

12. Ho, M., Post, C.M., Donahue, L.R., Lidov, H.G.W., Bronson, R.T., Goolsby, H., Watkins, S.C., Cox, G.A., and Brown, R.H., Jr. (2004). Disruption of muscle membrane and phenotype divergence in two novel mouse models of dysferlin deficiency. Hum. Mol. Genet. *13*, 1999–2010.

13. Lostal, W., Bartoli, M., Bourg, N., Roudaut, C., Bentaïb, A., Miyake, K., Guerchet, N., Fougerousse, F., McNeil, P., and Richard, I. (2010). Efficient recovery of dysferlin deficiency by dual adeno-associated vector-mediated gene transfer. Hum. Mol. Genet. *19*, 1897–1907.

14. Vafiadaki, E., Reis, A., Keers, S., Harrison, R., Anderson, L.V., Raffelsberger, T., Ivanova, S., Hoger, H., Bittner, R.E., Bushby, K., and Bashir, R. (2001). Cloning of the mouse dysferlin gene and genomic characterization of the SJL-Dysf mutation. Neuroreport *12*, 625–629.

15. Lu, Q.L., Mann, C.J., Lou, F., Bou-Gharios, G., Morris, G.E., Xue, S.A., Fletcher, S., Partridge, T.A., and Wilton, S.D. (2003). Functional amounts of dystrophin produced by skipping the mutated exon in the mdx dystrophic mouse. Nat. Med. *9*, 1009–1014.

16. Goyenvalle, A., Griffith, G., Babbs, A., El Andaloussi, S., Ezzat, K., Avril, A., Dugovic, B., Chaussenot, R., Ferry, A., Voit, T., et al. (2015). Functional correction in mouse

models of muscular dystrophy using exon-skipping tricyclo-DNA oligomers. Nat. Med. *21*, 270–275.

17. Goyenvalle, A., Babbs, A., Powell, D., Kole, R., Fletcher, S., Wilton, S.D., and Davies, K.E. (2010). Prevention of dystrophic pathology in severely affected dystrophin/utrophin-deficient mice by morpholino-oligomer-mediated exon-skipping. Mol. Ther. *18*, 198–205.
18. Goyenvalle, A., Leumann, C., and Garcia, L. (2016). Therapeutic Potential of Tricyclo-DNA antisense oligonucleotides. J. Neuromuscul. Dis. *3*, 157–167.
19. Porensky, P.N., and Burghes, A.H.M. (2013). Antisense oligonucleotides for the treatment of spinal muscular atrophy. Hum. Gene Ther. *24*, 489–498.
20. Robin, V., Griffith, G., Carter, J.L., Leumann, C.J., Garcia, L., and Goyenvalle, A. (2017). Efficient SMN Rescue following Subcutaneous Tricyclo-DNA Antisense Oligonucleotide Treatment. Mol. Ther. Nucleic Acids *7*, 81–89.
21. Barthélémy, F., Blouin, C., Wein, N., Mouly, V., Courrier, S., Dionnet, E., Kergourlay, V., Mathieu, Y., Garcia, L., Butler-Browne, G., et al. (2015). Exon 32 skipping of dysferlin rescues membrane repair in patients' cells. J. Neuromuscul. Dis. *2*, 281–290.
22. Aartsma-Rus, A., Singh, K.H.K., Fokkema, I.F.A.C., Ginjaar, I.B., van Ommen, G.-J., den Dunnen, J.T., and van der Maarel, S.M. (2010). Therapeutic exon skipping for dysferlinopathies? Eur. J. Hum. Genet. *18*, 889–894.
23. Galli, G., Hofstetter, H., Stunnenberg, H.G., and Birnstiel, M.L. (1983). Biochemical complementation with RNA in the Xenopus oocyte: a small RNA is required for the generation of 3′ histone mRNA termini. Cell *34*, 823–828.
24. Müller, B., and Schümperli, D. (1997). The U7 snRNP and the hairpin binding protein: Key players in histone mRNA metabolism. Semin. Cell Dev. Biol. *8*, 567–576.
25. Smith, H.O., Tabiti, K., Schaffner, G., Soldati, D., Albrecht, U., and Birnstiel, M.L. (1991). Two-step affinity purification of U7 small nuclear ribonucleoprotein particles using complementary biotinylated 2′-O-methyl oligoribonucleotides. Proc. Natl. Acad. Sci. USA *88*, 9784–9788.
26. De Angelis, F.G., Sthandier, O., Berarducci, B., Toso, S., Galluzzi, G., Ricci, E., Cossu, G., and Bozzoni, I. (2002). Chimeric snRNA molecules carrying antisense sequences against the splice junctions of exon 51 of the dystrophin pre-mRNA induce exon skipping and restoration of a dystrophin synthesis in Delta 48-50 DMD cells. Proc. Natl. Acad. Sci. USA *99*, 9456–9461.
27. Brun, C., Suter, D., Pauli, C., Dunant, P., Lochmüller, H., Burgunder, J.M., Schümperli, D., and Weis, J. (2003). U7 snRNAs induce correction of mutated dystrophin pre-mRNA by exon skipping. Cell. Mol. Life Sci. *60*, 557–566.
28. Gorman, L., Suter, D., Emerick, V., Schümperli, D., and Kole, R. (1998). Stable alteration of pre-mRNA splicing patterns by modified U7 small nuclear RNAs. Proc. Natl. Acad. Sci. USA *95*, 4929–4934.
29. Goyenvalle, A., Vulin, A., Fougerousse, F., Leturcq, F., Kaplan, J.C., Garcia, L., and Danos, O. (2004). Rescue of dystrophic muscle through U7 snRNA-mediated exon skipping. Science *306*, 1796–1799.
30. Wein, N., Avril, A., Bartoli, M., Beley, C., Chaouch, S., Laforêt, P., Behin, A., Butler-Browne, G., Mouly, V., Krahn, M., et al. (2010). Efficient bypass of mutations in dysferlin deficient patient cells by antisense-induced exon skipping. Hum. Mutat. *31*, 136–142.
31. Consortium, T.U.; The UniProt Consortium (2017). UniProt: the universal protein knowledgebase. Nucleic Acids Res. *45* (D1), D158–D169.
32. Fu, X.D., and Ares, M., Jr. (2014). Context-dependent control of alternative splicing by RNA-binding proteins. Nat. Rev. Genet. *15*, 689–701.
33. Fairbrother, W.G., Yeh, R.-F., Sharp, P.A., and Burge, C.B. (2002). Predictive identification of exonic splicing enhancers in human genes. Science *297*, 1007–1013.
34. Fairbrother, W.G., Yeo, G.W., Yeh, R., Goldstein, P., Mawson, M., Sharp, P.A., and Burge, C.B. (2004). RESCUE-ESE identifies candidate exonic splicing enhancers in vertebrate exons. Nucleic Acids Res. *32*, W187–W190.
35. Garcia, L., Furling, D., Beley, C., and Voit, T. July 2015. Modified U7 snRNAs for treatment of neuromuscular diseases. US patent 9,080,170 B2, filed March 17, 2011, and granted July 14, 2015.
36. Gruber, A.R., Lorenz, R., Bernhart, S.H., Neuböck, R., and Hofacker, I.L. (2008). The Vienna RNA websuite. Nucleic Acids Res. *36*, W70–W74.
37. Henriques, S.F., Patissier, C., Bourg, N., Fecchio, C., Sandona, D., Marsolier, J., and Richard, I. (2018). Different outcome of sarcoglycan missense mutation between human and mouse. PLoS ONE *13*, e0191274.
38. Bartoli, M., Gicquel, E., Barrault, L., Soheili, T., Malissen, M., Malissen, B., Vincent-Lacaze, N., Perez, N., Udd, B., Danos, O., and Richard, I. (2008). Mannosidase I inhibition rescues the human α-sarcoglycan R77C recurrent mutation. Hum. Mol. Genet. *17*, 1214–1221.
39. Stefanovic, B., Hackl, W., Lührmann, R., and Schümperli, D. (1995). Assembly, nuclear import and function of U7 snRNPs studied by microinjection of synthetic U7 RNA into Xenopus oocytes. Nucleic Acids Res. *23*, 3141–3151.
40. Grimm, C., Stefanovic, B., and Schümperli, D. (1993). The low abundance of U7 snRNA is partly determined by its Sm binding site. EMBO J. *12*, 1229–1238.
41. Benchaouir, R., Meregalli, M., Farini, A., D'Antona, G., Belicchi, M., Goyenvalle, A., Battistelli, M., Bresolin, N., Bottinelli, R., Garcia, L., and Torrente, Y. (2007). Restoration of human dystrophin following transplantation of exon-skipping-engineered DMD patient stem cells into dystrophic mice. Cell Stem Cell *1*, 646–657.
42. Goyenvalle, A., Babbs, A., van Ommen, G.-J.B., Garcia, L., and Davies, K.E. (2009). Enhanced exon-skipping induced by U7 snRNA carrying a splicing silencer sequence: Promising tool for DMD therapy. Mol. Ther. *17*, 1234–1240.
43. Goyenvalle, A., Babbs, A., Wright, J., Wilkins, V., Powell, D., Garcia, L., and Davies, K.E. (2012). Rescue of severely affected dystrophin/utrophin-deficient mice through scAAV-U7snRNA-mediated exon skipping. Hum. Mol. Genet. *21*, 2559–2571.
44. Bish, L.T., Sleeper, M.M., Forbes, S.C., Wang, B., Reynolds, C., Singletary, G.E., Trafny, D., Morine, K.J., Sanmiguel, J., Cecchini, S., et al. (2012). Long-term restoration of cardiac dystrophin expression in golden retriever muscular dystrophy following rAAV6-mediated exon skipping. Mol. Ther. *20*, 580–589.
45. Vulin, A., Barthélémy, I., Goyenvalle, A., Thibaud, J.-L., Beley, C., Griffith, G., Benchaouir, R., le Hir, M., Unterfinger, Y., Lorain, S., et al. (2012). Muscle function recovery in golden retriever muscular dystrophy after AAV1-U7 exon skipping. Mol. Ther. *20*, 2120–2133.
46. Mendell, J.R., Shilling, C., Leslie, N.D., Flanigan, K.M., al-Dahhak, R., Gastier-Foster, J., Kneile, K., Dunn, D.M., Duval, B., Aoyagi, A., et al. (2012). Evidence-based path to newborn screening for Duchenne muscular dystrophy. Ann. Neurol. *71*, 304–313.
47. Sanjana, N.E., Shalem, O., and Zhang, F. (2014). Improved vectors and genome-wide libraries for CRISPR screening. Nat. Methods *11*, 783–784.
48. Dull, T., Zufferey, R., Kelly, M., Mandel, R.J., Nguyen, M., Trono, D., and Naldini, L. (1998). A third-generation lentivirus vector with a conditional packaging system. J. Virol. *72*, 8463–8471.
49. Zufferey, R., Dull, T., Mandel, R.J., Bukovsky, A., Quiroz, D., Naldini, L., and Trono, D. (1998). Self-inactivating lentivirus vector for safe and efficient in vivo gene delivery. J. Virol. *72*, 9873–9880.
50. Xiao, X., Li, J., and Samulski, R.J. (1998). Production of high-titer recombinant adeno-associated virus vectors in the absence of helper adenovirus. J. Virol. *72*, 2224–2232.
51. Dias Florencio, G., Precigout, G., Beley, C., Buclez, P.-O., Garcia, L., and Benchaouir, R. (2015). Simple downstream process based on detergent treatment improves yield and in vivo transduction efficacy of adeno-associated virus vectors. Mol. Ther. Methods Clin. Dev. *2*, 15024.
52. Buclez, P.-O., Dias Florencio, G., Relizani, K., Beley, C., Garcia, L., and Benchaouir, R. (2016). Rapid, scalable, and low-cost purification of recombinant adeno-associated virus produced by baculovirus expression vector system. Mol. Ther. Methods Clin. Dev. *3*, 16035.
53. Aartsma-Rus, A., Janson, A.A.M., Kaman, W.E., Bremmer-Bout, M., den Dunnen, J.T., Baas, F., van Ommen, G.J., and van Deutekom, J.C. (2003). Therapeutic antisense-induced exon skipping in cultured muscle cells from six different DMD patients. Hum. Mol. Genet. *12*, 907–914.